Quantum corrections to the ground state energy of inhomogeneous neutron matter

Aurel BULGAC 1,2 and Piotr MAGIERSKI 1,3 ¹Department of Physics, University of Washington, Seattle, WA 98195-1560, USA ² Max-Planck-Insitut für Kernphysik, Postfach 10 39 80, 69029 Heidelberg, GERMANY

³ Institute of Physics, Warsaw University of Technology, ul. Koszykowa 75, PL-00662, Warsaw, POLAND (December 2, 2024)

We estimate the quantum corrections to the ground state energy in neutron matter (which could be termed as well either shell correction energy or Casimir energy) at subnuclear densities, where various types of inhomogeneities (bubbles, rods, plates) are energetically favorable. We show that the magnitude of these energy corrections are comparable to the energy differences between various types of inhomogeneous phases. We discuss the dependence of these corrections on a number of physical parameters (density, filling factor, temperature, lattice distortions).

PACS numbers: 21.10.Dr, 21.65.+f, 97.60.Jd

The investigation of the nuclear matter in the neutron star crust below the saturation density leads to the consideration of exotic shapes of the nuclei immersed in a neutron gas. It was realized long ago [1] that when the nuclei in dense matter occupy more than half of the space it is energetically favorable to "turn the nuclei inside out" and form a bubble phase [2–4]. To date a large number of calculations have been performed pertaining to the structure of the neutron star crust. The liquid drop model or the Thomas–Fermi approximation calculations [5-11] predict rather small energy differences between different phases, of the order of a few keV/fm^3 . (N.B. even though we often refer to energy, we actually mean energy density.). Apparently an agreement has been reached concerning the existence of the following chain of phase changes as the density is increasing: nuclei \rightarrow rods \rightarrow plates \rightarrow tubes \rightarrow bubbles \rightarrow uniform matter. The density range for these phase transitions is $0.04 - 0.1 \, fm^{-3}$ [9,10]. Moreover, it was established that these phases exist up to temperatures of about 10MeV [5]. At densities of the order of several nuclear densities the quark degrees of freedom get unlocked and the formation of various quark matter droplets embedded in nuclear matter becomes then energetically favorable [12].

The appearance of different phases is attributed to the interplay between the Coulomb and surface energies. Since most of the published works were based on the minimization of some density functional in a single Wigner-Seitz cell, the calculation of the shell correction or Casimir energy has been omitted. In Hartree-Fock calculations [13] these quantum corrections to the ground state energy of neutron matter are obviously automatically incorporated. The Hartree-Fock calculations performed so far were limited to "spherical Wigner-Seitz cells", which is arguably a reasonable approximation for the "nuclei in neutron gas" phase only. To our knowledge there exist only one study on this subject where the shell effects due to the bound nucleons only however (mainly protons) have been taken into account [14]. It was determined that the shell correction energy is smaller than the energy difference between different phases and it was thus concluded that quantum corrections to the ground state energy will not lead to any qualitative changes in the sequence of the nuclear shape transitions in the neutron star crust.

Our goal is to reach a comprehensive understanding of the so called shell correction or Casimir energy in neutron stars. There is no well established terminology for the energy corrections we are considering here, even though the problem has been addressed before to some extent by other authors. In the case of finite systems, the energy difference between the true binding energy and the liquid drop energy of a given system is typically referred to as shell correction energy. In field theory a somewhat similar energy appears, due to various fluctuation induced effects and it is generically referred to as the Casimir energy [15]:

$$E_{Casimir} = \int_{-\infty}^{\infty} d\varepsilon \varepsilon [g(\varepsilon, \mathbf{l}) - g_0(\varepsilon)], \tag{1}$$

where $g_0(\varepsilon)$ is the density of states per unit volume for the fields in the absence of any objects, $q(\varepsilon, \mathbf{l})$ is the density of states per unit volume in the presence of some "foreign" objects, such as plates, spheres, etc., and 1 is an ensemble of geometrical parameters describing these objects and their relative geometrical arrangement. A similar formula can be written for neutron matter energy

$$E_{nm} = \int_{-\infty}^{\mu} d\varepsilon \varepsilon g(\varepsilon, \mathbf{l}) - \int_{-\infty}^{\mu_0} d\varepsilon \varepsilon g_0(\varepsilon, \mathbf{l}), \tag{2}$$

with the notable difference in the upper integration limit. In the above equation $q_0(\varepsilon, \mathbf{l})$ stands for the Thomas-Fermi or liquid drop density of states of the inhomogeneous phase and $g(\varepsilon, \mathbf{l})$ for the true quantum density of states in the presence of inhomogeneities. The parameters: μ and μ_0 are determined from the requirement that the system has a given average density

$$\rho = \int_{-\infty}^{\mu} d\varepsilon g(\varepsilon, \mathbf{l}) = \int_{-\infty}^{\mu_0} d\varepsilon g_0(\varepsilon, \mathbf{l}). \tag{3}$$

Since in infinite matter the presence of various inhomogeneities does not lead to the formation of discrete levels, one might expect to refer to corresponding energy correction for neutron matter as the Casimir energy. In Ref. [14] the authors computed a somewhat different quantity however, than the one we are interested in this work, the correction to the ground state energy arising from existence of almost discrete levels inside a nucleus in an infinite medium. Strictly speaking these levels are not discrete, but form narrow energy bands due to the tunneling between neighboring nuclei. The effects we shall consider here arise from the "outside" states, which is in complete analogy with the procedure for computing the Casimir energy. As we shall show, these energy corrections, arising from the existence of these truly delocalized states, are larger than those considered in Ref. [14]. We have considered similar issues earlier in finite systems and to some extent in infinite 2-dimensional systems as well in Refs. [16,17].

In order to better appreciate the nature of the problem we are addressing in this work, let us consider the following situation. Let us imagine that two spherical identical bubbles have been formed in an otherwise homogeneous neutron matter. For the sake of simplicity, we shall assume that the bubbles are completely hollow. We shall sidestep the question of stability of each bubble for the moment and assume that they are stable and rigid as well. We shall ignore the role of long range forces, namely the Coulomb interaction in the case of neutron stars, as their main contribution is to the smooth, liquid drop or Thomas–Fermi part of the total energy. Under such circumstances one can ask the following apparently innocuous question: "What determines the most energetically favorable arrangement of the two bubbles?" According to a liquid drop model approach (completely neglecting for the moment the possible stabilizing role of the Coulomb forces) the energy of the system should be insensitive to the relative positioning of the two bubbles. A similar question was raised in condensed matter studies, concerning the interaction between two impurities in an electron gas. In the case of two "weak" and point-like impurities the dependence of the energy of the system as a function of the relative distance between the two impurities a is given by (spin coordinates are not displayed)

$$E(\mathbf{a}) = \frac{1}{2} \int d\mathbf{r}_1 \int d\mathbf{r}_2 V_1(\mathbf{r}_1) \chi(\mathbf{r}_1 - \mathbf{r}_2 - \mathbf{a}) V_2(\mathbf{r}_2), \quad (4)$$

where $\chi(\mathbf{r}_1 - \mathbf{r}_2 - \mathbf{a})$ is the Lindhard response function of a homogeneous Fermi gas and $V_1(\mathbf{r}_1)$ and $V_2(\mathbf{r}_2)$ are the potentials describing the interaction between impurities and the surrounding electron gas. At large distances $k_F a \gg 1$ this expression leads to the Ruderman–Kittel interaction [18,19]:

$$E(\mathbf{a}) \propto \frac{\hbar^2}{2mk_F a^3} \cos(2k_F a),$$
 (5)

where k_F is the Fermi wave vector and m is the fermion mass

$$\mu = \frac{\hbar^2 k_F^2}{2m}.\tag{6}$$

This asymptotic behavior is valid only for point–like impurities, when $k_FR \ll 1$, and where R stands for the radius of the two impurities. This condition is typically violated for either nuclei embedded in a neutron gas or bubbles, when typically $k_FR \gg 1$. As we shall show, in the case of large "impurities" (when $k_FR \gg 1$) the interaction energy changes in a rather dramatic manner. If one replaces the "weak" impurities with "strong" point–like impurities, only the magnitude of the interaction changes at large distances, but not the form [17]. The Ruderman–Kittel interaction is a pure quantum in character, and any "noise" (e.g. temperature) leads to a quick disappearance of the oscillatory behavior and with it of the power law character, and the regular Debye screening (which is exponential in character) sets in instead.

The lesson one can learn from this analysis however, is that quantum corrections are most likely responsible for the interaction of two bubbles/nuclei embedded in a Fermi gas and the form of the Ruderman-Kittel interaction suggests the most natural way to proceed. The argument of the cosine is nothing else but the classical action in units of \hbar of the bouncing periodic orbit between the two impurities. The exact form and magnitude of the coefficient in front of the cosine can be obtained in a semiclassical approximation only after a careful estimation of the leading order correction to the leading semiclassical result. Using the 3-dimensional extension of the semiclassical approximation to the so called small disks problem [20], we were to obtain a significantly simpler and more transparent derivation of this interaction than the original derivation [19] as follows. The correction to the single-particle propagator, which depends on the presence of the two weak widely separated point-like impurities $(R/a \ll 1 \text{ and } k_F R \ll 1)$ is

$$\delta G(\mathbf{r}, \mathbf{r}', k) \propto G_0(\mathbf{r}, \mathbf{r}_1, k) G_0(\mathbf{r}_1, \mathbf{r}_2, k) G_0(\mathbf{r}_2, \mathbf{r}', k)$$

$$+ G_0(\mathbf{r}, \mathbf{r}_2, k) G_0(\mathbf{r}_2, \mathbf{r}_1, k) G_0(\mathbf{r}_1, \mathbf{r}', k), \quad (7)$$

where

$$G_0(\mathbf{r}_1, \mathbf{r}_2, k) = \frac{\exp(ik|\mathbf{r}_1 - \mathbf{r}_2|)}{4\pi|\mathbf{r}_1 - \mathbf{r}_2|}$$
(8)

is the free single—particle propagator. Since only "periodic orbits" contribute to the density of states, the correction to the density of states, due to the presence of the two impurities and which depends on their relative separation only is given by

$$\delta g(k, |\mathbf{r}_1 - \mathbf{r}_2|) \propto -\frac{1}{\pi} \text{Im} \left[\frac{\exp(2ik|\mathbf{r}_1 - \mathbf{r}_2|)}{(4\pi|\mathbf{r}_1 - \mathbf{r}_2|)^2} \right]$$
 (9)

and the corresponding correction to the ground state energy is given by the obvious formula

$$\delta \mathcal{E}(|\mathbf{r}_{1} - \mathbf{r}_{2}|) \propto \int_{k \leq k_{F}} \frac{d^{3}k}{(2\pi)^{3}} \frac{\hbar^{2}k^{2}}{2m} \delta g(k, |\mathbf{r}_{1} - \mathbf{r}_{2}|)$$

$$\propto \frac{\cos(2k_{F}|\mathbf{r}_{1} - \mathbf{r}_{2}|)}{|\mathbf{r}_{1} - \mathbf{r}_{2}|^{3}}.$$
(10)

Only the leading term in the limit $|\mathbf{r}_1 - \mathbf{r}_2| \to \infty$ is explicitly shown here. The proportionality coefficient is naturally determined by the impurity strength.

The formation of various inhomogeneities in an otherwise uniform Fermi gas can be characterized by several natural dimensional parameters, $k_F a \gg 1$, where as above a is a characteristic separation distance between two such inhomogeneities, $k_F R \gg 1$, where R is a characteristic size of such an inhomogeneity, and $k_F s \approx 1$, where s is a typical "skin" thickness of such objects. The fact that the first two parameters, $k_F a$ and $k_F R$, are both very large makes a semiclassical approach natural. Since the third parameter, $k_F s$, is never too large or too small, one might be tempted to discard a semiclassical treatment of the entire problem altogether. However, there is a large body of evidence pointing towards the fact that even though this parameter in real systems is of order unity, the approximation $k_F s \ll 1$, which we shall adopt in this work, is surprisingly accurate [21]. Moreover the corrections arising from considering $k_F s = \mathcal{O}(1)$ should lead to an overall energy shift mainly, which is largely independent of the separation among various objects embedded in a Fermi gas. On one hand, this type of shift can be accounted for in principle in a correctly implemented liquid drop model or Thomas-Fermi approximation. On the other hand, the semiclassical corrections to the ground state energy arising from the relative arrangement of various inhomogeneities have to be computed separately, as they have a different physical nature. We are thus lead to the natural assumption that a simple hard-wall potential model for various types of inhomogeneities appearing in a neutron Fermi gas is a reasonable starting point to estimate quantum corrections to the ground state energy, see Refs. [16,17,21,22] and earlier references therein. We shall refer to these quantum corrections to the energy as shell effects in the rest of the paper. One might expect that such simplifications will result in an overestimation of the magnitude of shell effects, but the qualitative pattern should remain the same.

We shall consider spherical bubble–like, rod–like and plate–like phases only here and we shall estimate the shell correction or Casimir energy arising due to a regular arrangement of such inhomogeneities in an otherwise homogeneous neutron gas. One can distinguish two types of "bubbles": i) nuclei–like structures embedded in a neutron gas and ii) void–like structures. In the first case i), the single particle wave functions can be separated

into roughly two classes, those localized mostly inside the nuclei-like structures and those which are completely delocalized. A fermion in a delocalized state will spend some time inside the "nuclei" too, but since the potential experienced by a nucleon is deeper there, the local momentum is larger and thus the relative time and relative probability to find a nucleon in this region is smaller. One can approximately replace then the "nuclei" with an effective repulsive potential of roughly the same shape. In the case of a "bubble", when the probability to find a nucleon inside a "bubble" is reduced, again such an approximation appears as reasonable. The "nuclei" and "bubbles" we are referring to here, are not necessarily spherical, but could have the shape of a rod or plate as well. There are of course a number of "resonant" delocalized states, whose amplitude behaves in a manner just opposite to the one we have described here. However, the number of such "resonant" states is typically small and we thus do not expect large effects due to them. Moreover, since such states are concentrated mostly inside a "nucleus" or a "bubble" one does not expect them to affect in a major way the relative positioning of two "nuclei" or two "bubbles". Nevertheless, these are some issues, which certainly deserve more scrutiny in the future, even though we hardly expect that a more comprehensive analysis will lead to qualitative changes of our conclusions. In all these phases the shell effects depend on the structure and stability of periodic orbits in the system [21]. Except for the plate-like nuclei phase, where the shell energy can be computed exactly, for other geometries one should calculate the contribution from all periodic orbits. This is rather tedious task, since they proliferate exponentially as a function of their length [23], and moreover this is not really necessary to perform. If one is interested in the gross structure only of the shell effects, the contribution of the shortest periodic orbits should suffice for defining the gross shell structure. (We remind the reader, in an infinite medium there are really no shells as in a finite system, but we refer to the corresponding effects in this manner only, due to their similar origin because of the appearance of periodic orbits.) Since the contribution of any given periodic orbit leads to an oscillatory contribution to the density of states, with a smaller period the longer is the trajectory, any energy averaging over the spectrum, and in particular a finite temperature as well, will leave only the contributions due to the shortest periodic orbits. Moreover, since the geometry of the rod-like and spherical phases admit only unstable (hyperbolic) orbits, the longer the orbits, the lesser their contribution is, due their decreased stability.

The simplest system consist of plate-like nuclei with the neutron gas filling the space between slabs. The shell energy for this system per unit volume can be easily evaluated:

$$\frac{E_{shell}}{L^3} = \frac{E - E_{Weyl}}{L^3},\tag{11}$$

where the exact and the Weyl (smooth) energy [24] per unit volume are given by

$$\frac{E}{L^{3}} = \frac{2}{L^{3}} \frac{\hbar^{2}}{2ma^{2}} \frac{\pi^{3}}{2} \left(\frac{L}{a}\right)^{2} \left[\frac{1}{4} \left(\frac{k_{F}a}{\pi}\right)^{4} N\right] \qquad (12)$$

$$-\frac{N(N+1)(2N+1)(3N^{2}+3N-1)}{120},$$

$$\frac{E_{Weyl}}{L^{3}} = \frac{2}{L^{3}} \frac{\hbar^{2}}{2ma^{2}} \frac{\pi^{3}}{2} \left(\frac{L}{a}\right)^{2} \left[\frac{1}{5} \left(\frac{k_{F}a}{\pi}\right)^{5}\right]$$

$$-\frac{1}{8} \left(\frac{k_{F}a}{\pi}\right)^{4}.$$
(13)

In the above formula

$$N = \operatorname{Int}\left[\frac{k_F a}{\pi}\right] \tag{14}$$

stands for the integer part of the argument in the square brackets, and a=L-2R is the distance between slabs and R is the half of the width of the slab. Here L^3 is the volume of an elementary (cubic) cell and the factor '2' in front stands for the two spin states. Using these formulas one can show that the shell correction energy has the behavior

$$\frac{E_{shell}}{L^3} = \frac{\hbar^2 k_F^3}{48aLm} G\left(\frac{k_F a}{\pi}\right) \propto \frac{\rho_0}{a} = \frac{\rho}{L},\tag{15}$$

where G(x) is an approximate periodic function of its argument, for $x \geq 1$), $G(x+1) \approx G(x)$, with properties $G(x=n) \approx -1$ and $-1 \leq G(x) \leq 0.5$. Note that at small separations a the shell correction energy is attractive in character

The average density of the neutron gas (number of neutrons per unit volume) is determined by the following obvious relation

$$\rho_0 = 2\sum_{n=1}^{\infty} \int \frac{d^2k}{(2\pi)^2} \Theta\left(\mu - \frac{\hbar^2 k^2}{2m} - \frac{\hbar^2 n^2 \pi^2}{2ma^2}\right)$$

$$= \frac{2}{L^3} \frac{\pi}{4} \left(\frac{L}{a}\right)^2 \left[\left(\frac{k_F a}{\pi}\right)^2 N - \frac{N(N+1)(2N+1)}{6} \right].$$
(16)

Furthermore

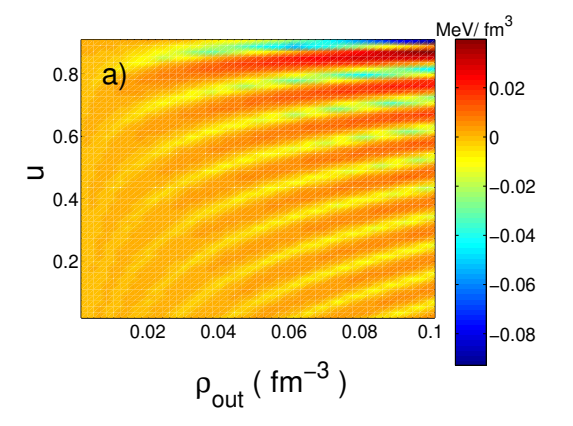
$$\rho_{out} = \frac{\rho_0}{v} \tag{17}$$

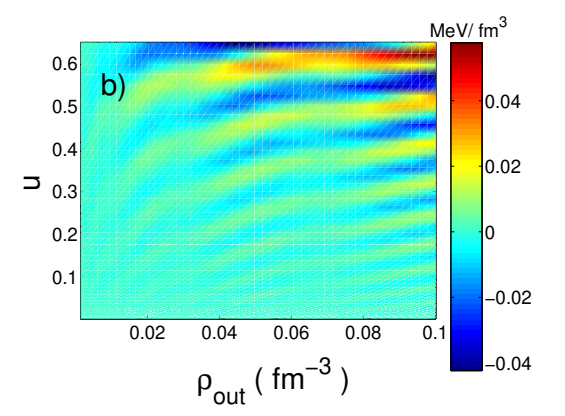
is the actual density of the neutron gas between the two slabs and

$$v = 1 - u = \frac{L - 2R_n}{L} \tag{18}$$

is the filling factor, which is the ratio of the occupied volume to the volume of the cell. One can show also that

$$\rho_0 = \rho_{Weyl} + \frac{k_F}{12La} F\left(\frac{k_f a}{\pi}\right),\tag{19}$$





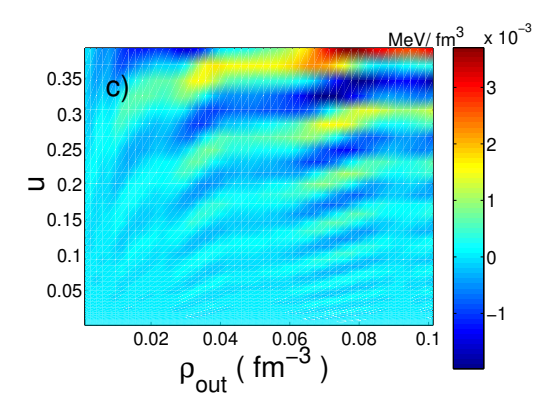


FIG. 1. The shell energy for the a) slab—like, b) rod—like and c) bubble—like phases respectively. The lattice constant has the corresponding values L=23,25,28fm.

where ρ_{Weyl} is the Weyl approximation to the density and $F(x+1) \approx F(x)$ is an approximate periodic function of its argument too, for $x \geq 1$, with properties $-1 \leq$ $F(x) \leq 0.5$ and F(x=n) = -1. This periodicity leads to the clear pattern of "valleys" $(k_F a = n\pi)$ and "ridges" $(k_F a \approx (n+1/2)\pi)$ in the profile of the shell energy shown in Fig. 1a. These features of the energy and density are naturally related to fact that these quantities are almost periodic functions in the classical action along the only periodic orbit in the system, i.e. in the variable $S=2k_Fa$.

In the case of rod–like and spherical voids we shall use the semiclassical theory in order to compute the shell energy. Since we are interested only in the "gross shell structure" we have to take into account a few of the shortest periodic orbits among the nearest neighbors only. The lengths of the shortest periodic orbits depend on the lattice type. In the following we will assume the simple cubic and simple square lattices for spherical and rod–like phases respectively. The expression for the shell energy density and the neutron density reads:

$$\frac{E_{shell}}{L^3} = \frac{1}{L^3} \int_0^{\mu} \varepsilon \sum_i g_{shell}(\varepsilon, L_i) d\varepsilon$$
 (20)

$$\rho_{out} = \frac{1}{L^3} \int_0^{\mu} \left[g_{Weyl}(\varepsilon) + \sum_i g_{shell}(\varepsilon, L_i) \right] d\varepsilon, \quad (21)$$

where $g_{shell}(\varepsilon, L_i)$ denotes the contribution to the level density due to the orbit L_i and g_{Weyl} is the smooth level density determined using the Weyl prescription [24].

For the rod-like phase we took into account four orbits of the length $2L_1 = 2(L-2R_1)$ and four orbits of the length $2L_2 = 2(L\sqrt{2} - 2R_2)$. Introducing longer orbits did not lead to noticeable changes in the patterns presented here. Hence the shell energy per volume is equal to:

$$\frac{E_{shell}}{L^3} = \frac{1}{L^3} \int_0^{\mu} \varepsilon \sum_{i=1}^2 A_i g_{shell}(\varepsilon, L_i) d\varepsilon, \tag{22}$$

where $A_1 = A_2 = 4$ and the chemical potential μ is determined by the condition:

$$\rho_{out} = \rho_{Weyl} + \frac{1}{L^3} \int_0^{\mu} \sum_{i=1}^2 A_i g_{shell}(\varepsilon, L_i) d\varepsilon.$$
 (23)

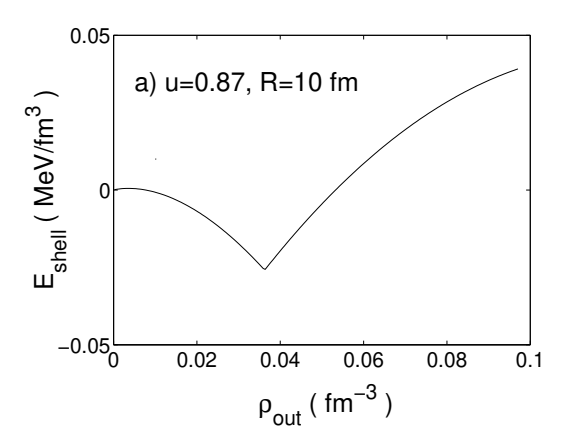
A periodic orbit of the type considered by us gives actually a contribution with a factor 1/2, since only half of it belongs to a particular elementary cell. Because there are two spin states, and thus eight orbits in total, each type of orbit eventually is weighted by four. The density of states was evaluated using the convolution of the exact 1-dimensional density of states and the density of states given by Gutzwiller trace formula for the 2-dimensional system of disks, which is the cross section of the rod-like system we are interested in. In some cases such a procedure can lead to spurious contributions, which are however rather easy to single out, see Refs. [25]. For a given periodic orbit of length $2L_i$, the shell correction to the density of states is given by the following expression

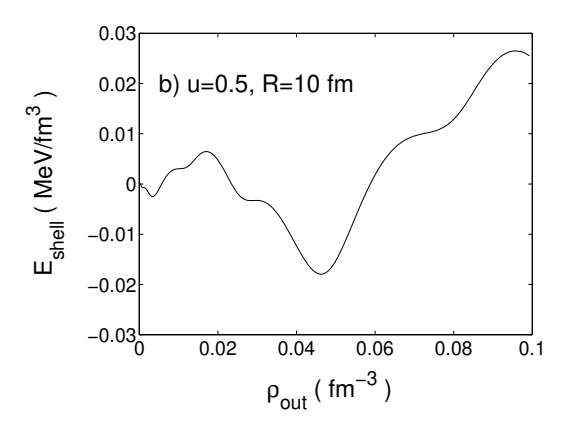
$$g_{shell}(\varepsilon, L_i) = \frac{mL}{4\hbar^2 k} \times$$

$$\sum_{n=1}^{\infty} \frac{nkL_i[J_0(2nkL_i) - J_2(2nkL_i)] + J_1(2nkL_i)}{n \sinh n\kappa_i},$$
(24)

where the summation is over repetitions of this orbit and

$$\varepsilon = \frac{\hbar^2 k^2}{2m}.\tag{25}$$





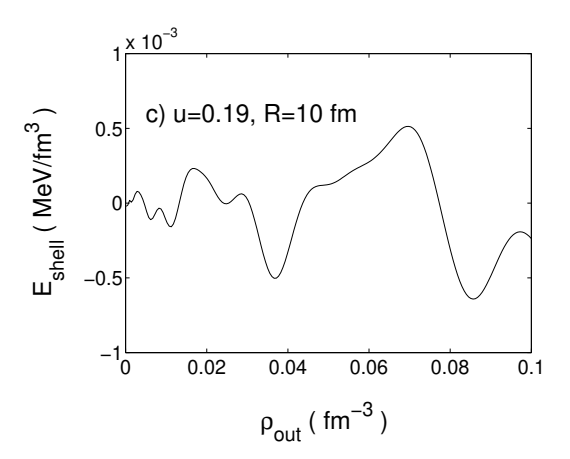


FIG. 2. The same as in the Figs. 1 but for fixed values of the anti–filling factor u. R is the separation between the voids.

The explicit form of the shell energy and of the fluctuating part of the density reads:

$$\frac{E_{shell}}{L^3} = \frac{1}{L^3} \frac{\hbar^2 k_F^2}{2m} \frac{1}{4} \sum_{i=1}^2 A_i \frac{L}{L_i} \times \sum_{n=1}^{\infty} \frac{\left[J_2(2nk_F L_i) - nk_F L_i J_3(2nk_F L_i) \right]}{n^2 \sinh(n\kappa_i)}$$
(26)

$$\rho_{out} = \rho_{Weyl} + \frac{k_F}{4L^2} \sum_{i=1}^{2} A_i \sum_{n=1}^{\infty} \frac{J_1(2nk_F L_i)}{n \sinh(n\kappa_i)}.$$
 (27)

The parameter κ_i determines the stability of the orbit L_i :

$$\kappa_i = \ln\left[1 + \frac{L_i}{R} + \sqrt{\frac{L_i}{R}\left(\frac{L_i}{R} + 2\right)}\right]. \tag{28}$$

The shell energy as a function of the anti–filling factor (relative void volume) $u = \frac{\pi R^2}{L^2}$ and ρ_{out} is shown in Fig 1b. The shell energy has a smaller amplitude then in the case of the plate–like phase. This comes about because the periodic orbits are now hyperbolic in the plane perpendicular to the rods. Note however that the pattern of "valleys" and "ridges" looks very similar to the one for the slabs. This is because the main contribution due to the classical orbit of length $2L_1$ is the same. There are small interference effects caused by the orbit of length $2L_2$ however. Since it is longer, this second trajectory contributes with a smaller weight.

For the case of spherical voids there are 26 periodic orbits between nearest neighbors of three different lengths $2L_1 = 2(L-2R)$, $2L_2 = 2(L\sqrt{2}-R)$ and $2L_3 = 2(L\sqrt{3}-R)$. Thus the shell energy and density are equal to:

$$\frac{E_{shell}}{L^3} = \frac{1}{L^3} \int_0^{\mu} \varepsilon \sum_{i=1}^3 A_i g_{shell}(\varepsilon, L_i) d\varepsilon, \tag{29}$$

$$\rho_{out} = \rho_{Weyl} + \frac{1}{L^3} \int_0^{\mu} \sum_{i=1}^3 A_i g_{shell}(\varepsilon, L_i) d\varepsilon.$$
 (30)

The contribution due to one periodic orbit to the fluctuating part of the level density reads:

$$g_{shell}(\varepsilon, L_i) = \frac{mL_i}{2\pi\hbar^2 k} \sum_{i=1}^{\infty} \frac{\cos(2nkL_i)}{\sinh^2(n\kappa_i)}.$$
 (31)

Hence we get:

$$\frac{E_{shell}}{L^3} = \frac{1}{L^3} \frac{\hbar^2 k_F^2}{2m} \sum_{i=1}^3 \frac{A_i}{8\pi^2 (k_F L_i)^2} \times$$
(32)

$$\sum_{n=1}^{\infty} \frac{\left[2nk_F L_i \cos(2nk_F L_i) + (2n^2k_F^2 L_i^2 - 1)\sin(2nk_F L_i)\right]}{n^3 \sinh^2(n\kappa_i)},$$

$$\rho_{out} = \rho_{Weyl} + \frac{1}{L^3} \frac{1}{4\pi} \sum_{i=1}^3 A_i \sum_{n=1}^\infty \frac{\sin(2nk_F L_i)}{n \sinh^2(n\kappa_i)},\tag{33}$$

where $A_1=6$, $A_2=12$, $A_3=8$ respectively. The shell energy for the spherical phase is shown in Fig 1c. In this case the anti–filling factor is given by $u=\frac{4}{3}\frac{\pi R^3}{L^3}$. A stronger interference pattern due to the orbits L_2 and L_3 can be seen. The amplitude of the shell effects is also lower due to the greater instability of the orbit on one hand, and due to the smaller relative volume of the scatterers on the other hand.

In a similar manner one can obtain the interaction energy between two isolated bubbles at large separations $(a = L - 2R \gg R)$

$$E_{\circ\circ} \approx \frac{\hbar^2 k_F^2}{2m} \left(\frac{R}{a}\right)^2 \frac{2\sin(2k_F a)}{\pi^2}.$$
 (34)

When compared with the Ruderman–Kittel interaction one sees several notable differences, the most striking of them being the fact that now the interaction is inversely proportional to the square of the separation, instead of $1/a^3$ as in Eq. (5). In a recent paper [27] the Casimir energy for similar arrangements has been calculated using the semiclassical approximation. In the case of Casimir energy the situation is somewhat simple, since instead of two independent dimensionless parameters $k_F R$ and $k_F L$, only one dimensional parameter exists R/L. Thus the Casimir energy for two spheres has naturally the form

$$E_{\circ\circ}^{Cas} = \frac{\hbar c}{L} F\left(\frac{R}{L}\right),\tag{35}$$

with an unknown function F(x). A similar, but much stronger result can be obtained for the critical Casimir energy [28], where one can show that the theory is conformal invariant. The authors of Refs. [27] provide also a very compelling argument why the semiclassical approximation should be particularly accurate for the calculation of the Casimir energy in case of ideal metallic boundaries and they show that using only the single periodic orbit the Casimir energy for two spheres is given by

$$E_{\circ \circ}^{Cas} = -\frac{\pi^3 \hbar c R}{720 L^2},\tag{36}$$

and dismiss this result as being valid for large separations, since it contradicts their expectations that it should agree with the Casimir–Polder interaction [29]

$$E_{\circ\circ}^{CP} \propto -\frac{\hbar c R^6}{L^7}. (37)$$

The authors of Ref. [27] argue that the contributions arising from the diffractive paths discussed in Refs. [30], should eventually lead to additional contributions, which will cancel exactly this longer range interaction and in the end, the authors hope that the Casimir–Polder result will be retrieved. The difference between these two results for the Casimir energy is very similar to the difference

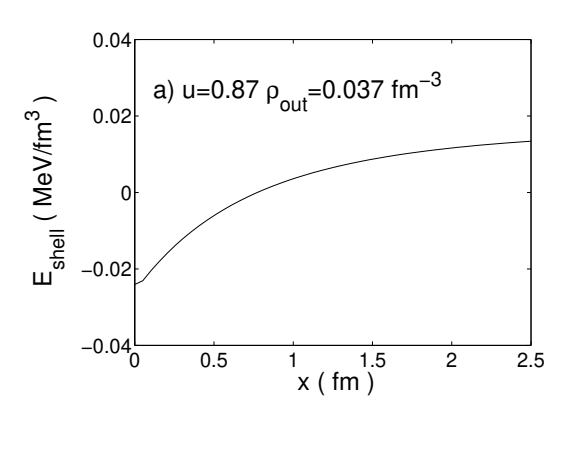
between the Ruderman–Kittel interaction between two point–like impurities $(k_FR \ll 1)$ and the interaction between two "fat" bubbles $(k_FR \gg 1)$ obtained above. In the case of "fat" bubbles, the contribution of diffractive orbits are exponentially small $(\propto \exp(-\alpha k_F R))$, where α is of order unity) [30], as one would naturally expect in the case when rays are a very good approximation to the wave phenomena. The resolution of this apparent conundrum lies in resolving the clear clash of limits. When $k_FR \to 0$ the "diffractive paths" are not suppressed anymore and an infinite number of them contribute to the scattering and thus to the propagator. It is notable that in the case of the critical Casimir effect, even longer range interactions $(\propto 1/a^{1+\epsilon})$, with very small ϵ 0 between two spheres are possible [28].

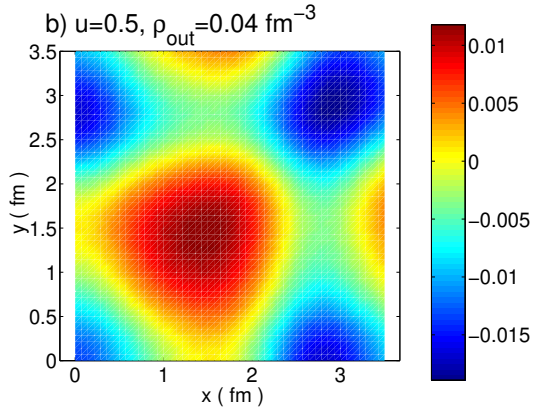
The structure of the shell energies shown in Figs. 1 indicates the existence of the optimal void sizes (with respect to the shell effects) for a given outside nucleon density. Note that for all phases and for $\rho_0 > 0.05 fm^{-3}$ the shell energy exhibits a remarkable softness toward adding additional neutrons to the system (the "valleys" and "ridges" are almost horizontal in Figs. 1). Hence one can conclude that once the size of the voids have been determined by minimization of the total energy of the system, an increase in the number of neutrons outside the voids will not affect much the shell energy of the system. However, the surface energy will be affected.

In the Fig. 2 we show the shell energies as a function of ρ_{out} for the optimal filling factors and nuclear radii determined in Ref. [8]. One can see that the amplitudes of the shell energies in the region $\rho_0 \approx 0.04-0.07$ are of the order of $0.03 MeV/fm^3$, $0.02 MeV/fm^3$ and $0.005 MeV/fm^3$ for plate–like, rod–like and bubble–like phases, respectively. There are usually one or two shallow shell energy minima for the density range $\rho_{out} > 0.03 fm^{-3}$. The minima are more pronounced in the case of spherical bubble–like phase mainly due to the stronger interference effects caused by longer orbits.

Once a phase is formed there is a positional order maintained by the Coulomb repulsion between spherical nuclei, rods or slabs [2-4,6,7,9]. Although the Coulomb energy is a smooth function of the void displacement [33], the shell energy is not. Since several different orbits contribute to the shell effects (except for slab-like phase) the displacement of a single bubble-like or rod-like void from its equilibrium position in the lattice will give rise to the interference effects. The interference pattern will depend on the type lattice. For the simple cubic and simple square lattices for spherical nuclei and rods, respectively, we show in the Fig. 3 the changes in the energy due to such "defects". For the plate-like system there is only one direction of displacement (we do not consider the shear mode) denoted by x perpendicular to the slab (Fig. 3a). Since the rod-like phase is a two-dimensional system, in the Fig 3b we have shown the shell energy as a function of two perpendicular displacements x and y.

They are perpendicular to the rods and point in the direction of the nearest neighbor. The same axes have been chosen for the spherical system although it will not exhaust all possible directions in the system. The behavior of the shell energy in this case is shown in Fig 3c.





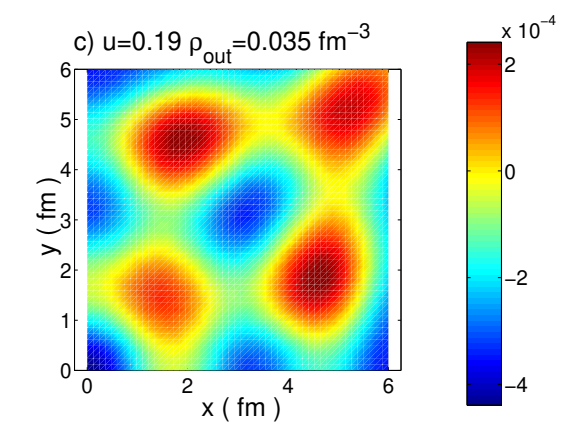


FIG. 3. The shell energy as a function of displacement of a single void in a lattice for a) plate–like, b) rod–like and c) bubble–like phases. The color bar at the right of each figure decodifies the value of each color in $MeVfm^3$ as in Figs. 1.

The structure of the shell energy surface as a function of a displacement depends on the lengths of the shortest periodic orbits. Except for the trivial plate—like phase, in the rod—like and spherical phase there exist directions into which is easier to locally deform the lattice.

In Fig. 4 we show the pattern of the energy changes induced by deforming the rod-like lattice. We considered only volume conserving deformations. The square lattice was stretched by a factor α in the x-direction, by a factor β in the y-direction and also the angle between the two axes has been changed to γ . In order to preserve the volume all these three parameters should satisfy the condition

$$\alpha\beta\sin\gamma = 1. \tag{38}$$

The case $\gamma = \pi/3$ correspond to the perfect triangular lattice.

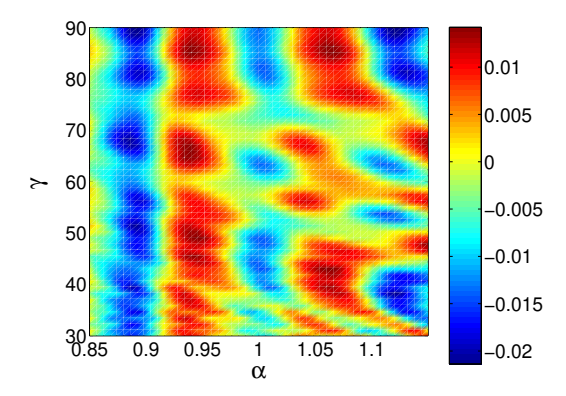


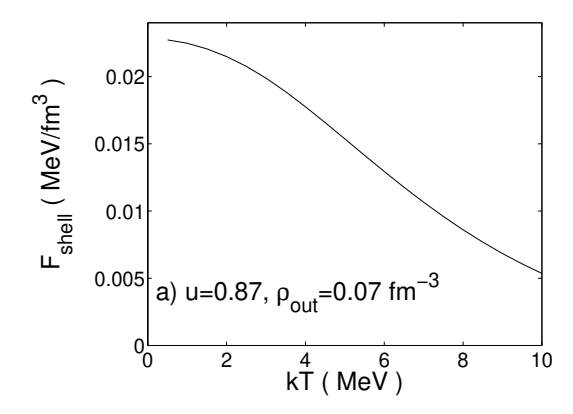
FIG. 4. The shell energy for a deformed rod–like lattice as a function of two independent deformation parameters α and γ . The color bar at the right of the figure decodifies the value of each color in $MeV fm^3$ as in Figs. 1.

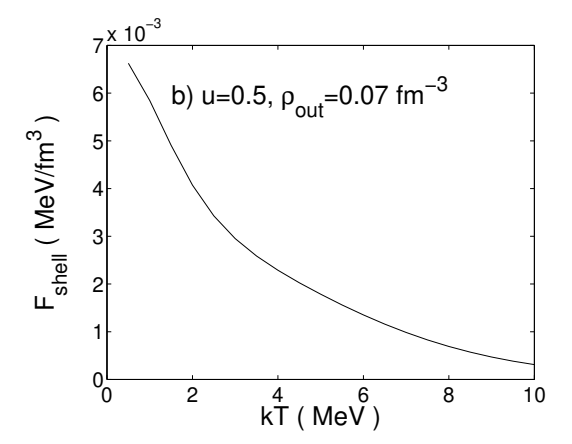
Increasing the temperature will weaken the shell effects. At sufficiently high temperatures the nuclear lattice will disappear. At smaller temperatures however, when the lattice can be regarded as frozen, the rise of the temperature will affect mainly shell effects in the neutron gas. In order to wash out completely the shell effects the temperature kT should be of the order of half of the distance between shells The spacing between two consecutive shells is determined by the length of the shortest orbit, a = L - 2R. Thus the energy distance between shells can be determined from the requirement: $2ka = 2\pi$ and is given by the expression:

$$\Delta E = \frac{\hbar^2 \pi^2}{2m(L - 2R)^2}.$$
 (39)

For the optimal filling factors and lattice constants of various phases obtained in Ref. [8] one obtains the following estimates for the critical temperature:

$$kT_c \approx 32 MeV$$
 for plate–like system,
 $kT_c \approx 19 MeV$ for rod–like system, (40)
 $kT_c \approx 12 MeV$ for spherical system.





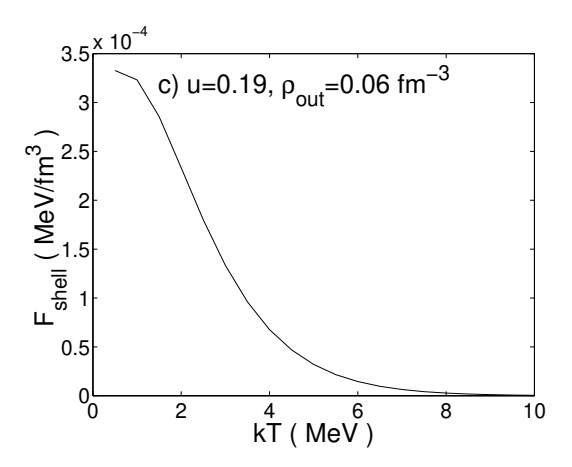


FIG. 5. The shell energy as a function of temperature at fixed u and ρ_{out} . a) plate–like phase, b) rod–like phase, c) bubble–like phase.

An accurate description of the shell effects as a function of the temperature can be obtained using the temperature averaged level density [21,26]:

$$g_{shell}(\varepsilon, T) = \sum_{p.o.} \frac{A_i \tau_{i,n}(T)}{\sinh \tau_{i,n}(T)} g_{shell}(\varepsilon, L_i), \tag{41}$$

where the sum is taken over all periodic orbits including the number of repetitions n of the orbit and

$$\tau_{i,n} = \frac{2\pi k T m n L_i}{\hbar^2 k}.$$
 (42)

Consequently the oscillating part of the free energy is given by the formula:

$$F_{shell} = \int_{0}^{\mu} \varepsilon g_{shell}(\varepsilon, T) d\varepsilon. \tag{43}$$

The results of calculations for different phases are shown in the Fig. 5. One can see that except for the spherical phase there is a tail, even for kT > 10 MeV. Since it was predicted that the phases do not exist for temperatures above 10 MeV [5], one can conclude that the thermal effects do not play a determining role.

Now at the end of this analysis we suspect that there are a lot of other effects, which might be relevant. We did not consider periodic orbits bouncing between three or more objects. An orbit bouncing between two bodies leads to a pairwise interaction. Orbits bouncing between three or more bodies would lead to genuine many body interactions. We have also considered only perfectly smooth objects. If one allows for some degree of corrugation of these surfaces, many more periodic orbits are likely to appear and that would lead to even more complicated interactions and more complicated interference patterns. The fact that corrugation can influence in a significant, perhaps major way, the Casimir energy, has already been predicted and measured experimentally [31]. The long range character of the interaction together with its oscillatory nature could very easily be at the origin of disorder, even at zero temperature. At finite temperature disorder is more likely to occur, due to entropic effects [16,17]. We did not consider here the role of pairing, which we expect however to lead to a certain flattening of the shell effects [16,17], which, however, should not be interpreted as disappearance of shell effects. Especially at subnuclear densities neutron pairing should be rather strong [32]. A completely different type of softness of these structures has been argued in Ref. [33], according to which the mantles of neutron stars resembles more liquid crystals than solids.

In the paper we have studied the shell effects in the neutron medium filled by different nuclear phases. To our knowledge this is the first approach which considers specifically the shell effects in the outside neutron gas and we aimed at discussing its basic features. Even though in principle Hartree–Fock calculations include in principle such effects already, the calculations performed so far [13] were too narrow in scope and did not address this issue specifically. Using semiclassical methods, we have analyzed the structure of the shell energy as a function of the density, filling factor, lattice distortions and temperature. We expect that our result overestimate somewhat the amplitude of the shell effects. However, the emerging qualitative overall picture should remain valid and further microscopic studies are highly desirable. The main

lesson one should remember from this work is that the amplitude of the shell energy effects is comparable with the energy differences between various phases determined in simpler liquid drop type models. This fact alone suggests that the inhomogeneous phase has perhaps an extremely complicated structure, maybe even completely disordered, with several types of shapes present at the same time.

The DOE financial support is gratefully acknowledged. This research was supported in part by the Polish Committee for Scientific Research (KBN) under Contract No. 2 P03B 040 14. AB thanks N.D. Whelan, O. Agam, T. Guhr and S.C. Creagh for discussions and correspondence concerning various aspects of the semiclassical approximation. PM thanks the Nuclear Theory Group for hosting his visit in Seattle. AB thanks the members of the Nuclear Theory Group at the Institute of Theoretical Physics in Warsaw for their hospitality. And last but not least, AB thanks W.A. Weidenmüller for being such a gracious host.

- G. Baym et al., Nucl. Phys. A175, 225 (1971).
- [2] D.G. Ravenhall et al., Phys. Rev. Lett. **50**, 2066 (1983).
- [3] M. Hashimoto et al., Prog. Theor. Phys. 71, 320 (1984).
- [4] K. Oyamatsu et al., Prog. Theor. Phys. 72, 373 (1984).
- [5] J.M. Lattimer et al., Nucl. Phys. A432, 646 (1985).
- [6] R.D. Wilson and S.E. Koonin, Nucl. Phys. A435, 844 (1985).
- [7] M. Lassaut et al., Astron. Astrophys. 183, L3 (1987).
- [8] K. Oyamatsu, Nucl. Phys. **A561**, 431 (1993).
- [9] C.P. Lorenz et al., Phys. Rev. Lett. **70**, 379 (1993).
- [10] C.J. Pethick and D.G. Ravenhall, Annu. Rev. Nucl. Part. Sci. 45, 429 (1995).
- [11] G. Watanabe et al., see Los Alamos e-print archive astroph/0001273.
- [12] H. Heiselberg et al., Phys. Rev. Lett. 70, 1355 (1992).
- [13] J.W. Negele and D. Vautherin, Nucl. Phys. A207, 298 (1973); P. Bonche and D. Vautherin, Nucl. Phys. A372, 496 (1981); Astron. Astrophys. 112, 268 (1982).
- [14] K. Oyamatsu, M. Yamada, Nucl. Phys. A578, 181 (1994).
- [15] M. Kardar and R. Golestanian, Rev. Mod. Phys. 71, 1233 (1999) and references therein.
- [16] Y. Yu et al., Phys. Rev. Lett. 84, 412 (2000).
- [17] A. Bulgac et al., in Proc. Intern. Work. on Collective excitations in Fermi and Bose systems, eds. C.A. Bertulani and M.S. Hussein (World Scientific, Singapore 1999), pp 44–61 and Los Alamos e–preprint archive, nucl-th/9811028.
- [18] M.A. Ruderman, C. Kittel, Phys. Rev. 96, 99 (1954).
- [19] A.L. Fetter and J.D. Walecka, Quantum Theory of Many Particle Systems, (McGraw-Hill, New York, 1971).
- [20] P.E. Rosenqvist et al., J. Phys. A 29, 5441 (1996).
- [21] M. Brack, R.K. Bhaduri, Semiclassical Physics, Addison

- Wesley Publishing Company, Inc. (1997)
- [22] A. Bulgac and C. Lewenkopf, Phys. Rev. Lett. 71, 4130 (1993).
- [23] H. Primack and Uzy Smilansky, Phys. Rev. Lett. 74, 4831 (1995); Los Alamos e-preprint archive, chaodyn/9907006 (1999), submitted to Phys. Rep.
- [24] R.T. Waechter, Proc. Camb. Phil. Soc. 72, 439 (1972); H.P. Baltes and E.R. Hilf, Spectra of Finite Systems, Wissenschaftsverlag, Mannheim, Wien, Zürich: Bibliographisches Institut, (1976).
- [25] J. Sakhr and N.D. Whelan, see Los Alamos e-preprint archive nlin.CD/0001051; R.K. Bhaduri et al., Phys. Rev. A 59, R911 (1999).
- [26] V.M. Kolomietz el., Sov. J. Nucl. Phys. 29, 758 (1979).
- [27] M. Schaden and L. Spruch, Phys. Rev. A 58, 935 (1998); Phys. Rev. Lett. 84, 459 (2000).
- [28] A. Hanke *et al.*, Phys. Rev. Lett. **81**, 1885 (1998) and references therein.
- [29] H.B.G. Casimir and D. Polder, Phys. Rev. 73, 360 (1948).
- [30] G. Vattay et al., Phys. Rev. Lett. 73, 2304 (1994); M. Henseler et al., Ann. Phys. 258, 29 (1997).
- [31] G.L. Klimchitskaya et al.. Phys. Rev. A 60, 3487 (1999);
 A. Roy et al., Phys. Rev. D 60, 111101(R) (1999).
- [32] V.A. Khodel et al., Nucl. Phys. **A598**, 390 (1996).
- [33] C.J. Pethick and A.Y. Potekhin, Phys. Lett. **B427**, 7 (1998).